

* email: schuetz@theory.phy.tu-dresden.de

Quantum algorithm for optical template recognition with noise filtering

Gernot Schaller and Ralf Schützhold*

Institut für Theoretische Physik, Technische Universität Dresden, D-01062 Dresden, Germany

We propose a probabilistic quantum algorithm that decides whether a monochrome picture matches a given template (or one out of a set of templates). As a major advantage to classical pattern recognition, the algorithm just requires a few incident photons and is thus suitable for very sensitive pictures (similar to the Elitzur-Vaidman problem). For a $2^n \times 2^m$ image, $\mathcal{O}(n+m)$ qubits are required. Using the quantum Fourier transform, it is possible to improve the fault tolerance of the quantum algorithm by filtering out small-scale noise in the picture. We have numerically simulated a quantum computer to demonstrate the applicability of the algorithm and to analyze its fault tolerance.

PACS numbers: 03.67.Lx, 03.67.-a.

I. INTRODUCTION

It is well known that quantum computers are suited to solving certain classes of problems much better than classical computers. A prominent example is Shor's algorithm [1] for factoring an integer number with an effort that grows polynomially in the number of its digits, which is believed to be classically impossible. A further impressive example is Grover's algorithm [2] for finding an item in an unsorted database: There, the effort grows only as the square-root \sqrt{N} of the number of database entries on a quantum computer, whereas it grows with N on a classical computer. In addition, there are further black box problems such as the Deutsch algorithm [3], the Deutsch-Josza algorithm [4] and others [5, 6, 7] (for an overview see e. g., [8]).

The possible speedup of quantum algorithms is essentially enabled by the feature of quantum parallelism. This parallelism permits to calculate with a superposition of states on a quantum computer, which is not possible on classical computers. The first quantum computers have already been constructed. For example, Shor's algorithm has been used on an NMR quantum computer to factorize the number 15 [9]. This is certainly not impressive if one considers the smallness of the number but nevertheless serves as a proof of principle.

However, there exists a plethora of further classically challenging problems such as e. g., pattern recognition [10], which can also benefit from the application of quantum algorithms [11, 12, 13, 14]. It has already been demonstrated that quantum parallelism can be exploited to identify and localize a regular simple pattern [15]. Here, we will present a probabilistic quantum algorithm that is capable of recognizing an image (even in the presence of noise) after shining a few photons on the picture. In contrast to previous pattern matching approaches (see, e. g., [13]), it does not require the copying of quantum states (which is only possible probabilistically) and enables a (probabilistically) non-destructive measurement, cf. [5].

II. PROBLEM DEFINITION

Following the problem description of [15], let us consider a rectangular $N_x \times N_y$ array of unit cells that may either be black (absorptive) or white (reflective). To allow for a binary representation, we will consider cases where the number of array cells in every dimension are powers of 2, i. e., $\log_2 N_{x/y} = n_{x/y}$ with integers $n_{x/y}$. Further-on, we will denote the pixels in the array that are reflective as **points**.

The problem consists of recognizing whether the pattern in the array matches a given template (for example, a letter of an alphabet). Note that this slightly differs from template matching discussed e. g., in [13, 14], where a template is to be found that optimally matches the given unknown quantum state. With using varying templates however, one can evidently establish a relation between these problems. The classical approach to measure the displayed pattern on the array would be to shine light (consisting of many, at least $\mathcal{O}\{N_x \times N_y\}$, photons) on the array and to measure absorption and transmission accordingly. However, in the case we consider here, the array is also assumed to be very sensitive (imagine, for example, a not yet developed film or a line of partially fluorescent ions in a Paul trap), such that each absorbed photon causes a certain amount of damage. Evidently, the classical measurement approach would significantly disturb the system.

One might worry that the momentum of the reflected photon (recoil) also disturbs the picture, but this effect will be extremely small if the mass of a pixel is sufficiently big. Alternatively, one might imagine the reflective pixels to be transparent and to place a mirror behind the array. Then, a quantum algorithm can cope with such a task: The feature of quantum parallelism can be exploited by storing the relevant information of the image in a quantum superposition state with using just a single photon and not (or only very little) destroying the image. The task is thus similar to the Elitzur-Vaidman problem [5], which allows for testing for the existence of an object without an energy-momentum exchange.

III. READ-OUT SCHEME

Generally, the coordinates (x, y) of a pixel in the image can be written in their binary representation

$$x = x_1 \otimes \dots \otimes x_{n_x} \quad y = y_1 \otimes \dots \otimes y_{n_y}, \quad (1)$$

where x_i and y_j denote the i -th and j -th bit of x and y , respectively, i. e., $x = x_1 2^{n_x-1} + x_2 2^{n_x-2} + \dots + x_{n_x}$. Regarding these coordinates (x, y) as control qubits $|x\rangle = |x_1\rangle|x_2\rangle\dots|x_{n_x}\rangle$, the photon probing the image can be entangled with the coordinates in the following way:

The photon passes through a series of quantum controlled refractors $R_{n_x}^x \dots R_1^x R_{n_y}^y \dots R_1^y$ that effectively displace the photon by defined distances Δx_i or Δy_i , if the control qubit $|x_i\rangle$ or $|y_i\rangle$ is in the state $|1\rangle$ and leave it unaffected if the control bit is in the state $|0\rangle$. By choosing the displacement of the refractor R_i^x as $\Delta x_i = 2^i \Delta x_0$ (and likewise for the other refractors R_i^y), the final displacement of the photon corresponds to the coordinates (x, y) which encode the position of a single image pixel.

In a laboratory setup, this could for example be realized by using a varying refractor thickness, see figure 1 left panel. For quantum controlled devices, one can generate use superposition states of several pixel positions in the image as control qubits. Storing these bits in a coherent superposition state containing all pixels with equal amplitudes, a single photon can be forced to interact simultaneously and uniformly with the complete array.

One should be aware that this causes a strong entanglement between the photon position and the control qubits. Thus, any measurement on the photon would affect the refractor control qubits as well and completely decohere them. The interaction of the photon with the image corresponds to absorption or reflection. In case of (perpendicular) reflection, the photon will reverse its original path (this is enforced by the entanglement with the refractor control qubits) and after passing through all refractors again, all information about the way of the photon (given that it was reflected) is lost. Thus, the entanglement with the control qubits is partially removed (quantum eraser) and we obtain a coherent superposition of the reflecting pixels (points). In the other case (absorption), the entanglement cannot be removed, and the algorithm fails – i. e., one has to send another photon if permitted by the fragility of the quantum array. As a formal simplification, one can consider the action of the configuration of the setup in figure 1 as a quantum black box:

$$\mathcal{B} : |x\rangle \otimes |y\rangle \otimes |0\rangle \rightarrow |x\rangle \otimes |y\rangle \otimes |f(x, y)\rangle, \quad (2)$$

which encodes the output in the characteristic function $f(x, y)$ of the image. The function $f(x, y)$ takes the value 1 if the pixel $x \otimes y$ is reflective (i. e., if $|x\rangle \otimes |y\rangle$ encodes a point) and 0 if the pixel is black (i. e., if the photon is absorbed). If the control qubits on the refractors are prepared in a superposition state (e. g., acting Hadamard

gates on each qubit), the characteristic function $f(x, y)$ of the image is tested for all pixels simultaneously

$$\mathcal{B} \left[\mathcal{H}^{(n_x)} |0^{(n_x)}\rangle \otimes \mathcal{H}^{(n_y)} |0^{(n_y)}\rangle \otimes |0\rangle \right] = \frac{1}{\sqrt{N_x N_y}} \sum_{x=0}^{N_x-1} \sum_{y=0}^{N_y-1} |x\rangle \otimes |y\rangle \otimes |f(x, y)\rangle. \quad (3)$$

Measuring the ancilla qubit (i. e., the existence of a reflected photon) and obtaining $|1\rangle$ as a result prepares the quantum state as an uniform superposition of all points in the image. The other outcome ($|0\rangle$) corresponds to the absorption of the photon and would lead to entanglement between the refractor control qubits and the image. Thus, with the outcome $|1\rangle$ (outgoing photon) one has prepared a quantum state (in the refractor control qubits) that is suitable for performing further calculations. Note that this scheme has the advantage that the image does not have to be loaded into a possibly fragile quantum memory (cf. [13, 14]).

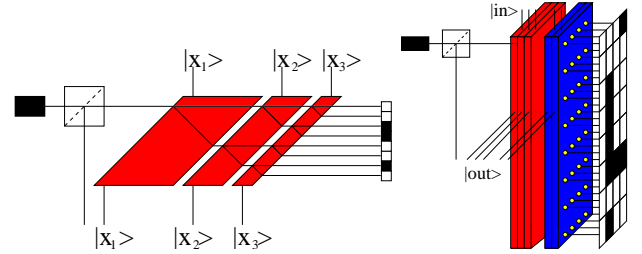


FIG. 1: [Color Online] **Left:** Illustration of a series of three quantum-controlled refractors required for an 8-pixel one-dimensional array. A photon created by the source (box in the left) passes the refractor series, interacts with the pixel array and takes – if reflected – the reverse path. Depending on the value of the control qubits $|x_i\rangle$, the refraction index of the medium is changed, which effectively produces a displacement of the photon. **Right:** Schematic representation of the two-dimensional configuration (exemplified for an 8×4 array). The first three refractors generate the displacement in x -direction (for 8 pixels) and the remaining two act in the y -direction (for 4 pixels).

IV. QUANTUM ALGORITHM

After extracting the superposition state containing all points of the image

$$|\Psi\rangle = \sum_{x=0}^{N_x-1} \sum_{y=0}^{N_y-1} \frac{f(x, y)}{\sqrt{M}} |x\rangle |y\rangle = \sum_{(x, y) \in \text{image}} \frac{|x, y\rangle}{\sqrt{M}}, \quad (4)$$

where $M < N_x N_y$ denotes the total number of points, one has to decide whether it corresponds to a given template. This can be done via an inverse application of Grovers algorithm:

Using an oracle function which yields 1 for the marked items and 0 otherwise, a Grover iteration generates a rotation in the two-dimensional sub-space of the Hilbert space spanned by the coherent superpositions of all numbers $|s\rangle$ on the one hand and the numbers of the marked items on the other hand. Using the characteristic function $f(x, y)$ of the image as an oracle, the Grover iterations rotate between the state $|\Psi\rangle$ in the above equation and the total superposition state $|s\rangle = \mathcal{H}^{(n_x)}|0^{(n_x)}\rangle \otimes \mathcal{H}^{(n_y)}|0^{(n_y)}\rangle$.

Since there are M solutions to this search problem,

$$R = \left\lceil \frac{\pi}{4} \sqrt{\frac{N_x N_y}{M}} \right\rceil \quad (5)$$

inverse Grover iterations will rotate the original state $|\Psi\rangle$ in Eq. (4) into the total superposition state $|s\rangle$, or at least close to it (discretization error, see below). After application of a Hadamard gate to each of the qubits, the resulting state would be $|0^{(n_x)}\rangle \otimes |0^{(n_y)}\rangle$. If the image indeed perfectly equals the template – i. e., if their characteristic functions coincide – and if the Grover iterations were assumed to be perfect (no discretization error), the state $|\Psi\rangle$ in Eq. (4) prepared after measuring the returning photon would be unitarily transformed into the final state $|0^{(n_x)}\rangle \otimes |0^{(n_y)}\rangle$. Consequently, a measurement in the computational basis would yield zeros for all bits.

If the image differs from the template and if the Grover iterations would yield a perfect rotation, the probability of ending up in the final state $|0^{(n_x)}\rangle \otimes |0^{(n_y)}\rangle$ would be given by the overlap of the characteristic functions of the template $f(x, y)$ and the image $f'(x, y)$

$$p = \frac{1}{MM'} \left| \sum_{x=0}^{N_x-1} \sum_{y=0}^{N_y-1} f(x, y) f'(x, y) \right|^2 \quad (6)$$

since all involved operations were unitary and hence probability conserving. Since this overlap determines how similar image and template are, measuring all qubits at the end and obtaining zero everywhere is a strong indication that the image equals the template or at least is very similar to it. Obtaining 1 somewhere, on the other hand, indicates that the image does not equal the template with high probability. As usual, the result can be made more decisive by repeating the whole algorithm. Note that due to the finite accuracy of the Grover rotation, even for perfect matches of the template and without any experimental inaccuracies, a probability $p = 1$ will not be obtained.

V. NOISE FILTERING

So far, the input state $|\Psi\rangle$ was assumed to be perfect. The basic algorithm described above can be improved using the quantum Fourier transform to reduce possible perturbations: As in classical pattern recognition, one

can perform a cutoff of large wave-numbers, which reduces noise such as pixel defects. In a quantum algorithm, such a cutoff can be realized via a measurement of an ancilla qubit which has been coupled to the control qubits: To this end, we introduce a unitary noisefilter operator

$$\mathcal{N}[|k_x\rangle \otimes |k_y\rangle \otimes |0\rangle] = |k_x\rangle \otimes |k_y\rangle \otimes \{\cos[\vartheta(k_x, k_y)]|1\rangle + \sin[\vartheta(k_x, k_y)]|0\rangle\}, \quad (7)$$

with a suitably chosen noisefilter function $\vartheta(k_x, k_y)$. Measuring the last register and obtaining $|1\rangle$ performs a cutoff in frequency space.

Let M_{tp} denote the number of template points and $M_{\text{im}} \approx M_{\text{tp}}$ the number of image points. Then, the quantum algorithm can be summarized as follows (compare also figure 2):

1. initialize the state vector with uniform superpositions in x and y as well as two ancilla qubits
 $|\Psi_1\rangle = \mathcal{H}^{(n_x)}|0^{n_x}\rangle \otimes \mathcal{H}^{(n_y)}|0^{n_y}\rangle \otimes |0\rangle \otimes |0\rangle$
2. apply the black box with the first ancilla qubit
 $|\Psi_2\rangle = \mathcal{B}|\Psi_1\rangle$
3. measure the first ancilla qubit and proceed after obtaining the outcome $|1\rangle$
 $|\Psi_3\rangle \stackrel{1}{=} M_{\text{im}}^{-1/2} \sum_{(x,y) \in \text{image}} |x\rangle \otimes |y\rangle \otimes |1\rangle \otimes |0\rangle$
4. perform quantum Fourier transform in $|x\rangle$ and $|y\rangle$
 $|\Psi_4\rangle = \mathcal{QFT}_{x,y}|\Psi_3\rangle$
5. apply noise filter operator with second ancilla
 $|\Psi_5\rangle = \mathcal{N}|\Psi_4\rangle$
6. measure the second ancilla qubit and proceed after obtaining the outcome $|1\rangle$
 $|\Psi_6\rangle \stackrel{1}{=} \sum_{k_x, k_y} \tilde{f}_{\text{cut}}(k_x, k_y) |k_x\rangle \otimes |k_y\rangle \otimes |1\rangle \otimes |1\rangle$
with $\tilde{f}_{\text{cut}}(k_x, k_y) = \tilde{f}(k_x, k_y) \cos[\vartheta(k_x, k_y)]$
7. perform inverse quantum Fourier transform
 $|\Psi_7\rangle = \mathcal{QFT}_{x,y}^\dagger|\Psi_6\rangle$
8. perform R inverse Grover iterations \mathcal{G}^{-1}
 $|\Psi_8\rangle = \mathcal{G}^{-R}|\Psi_7\rangle$
9. apply Hadamard gates on non-ancilla qubits
 $|\Psi_9\rangle = \mathcal{H}^{(n_x)} \otimes \mathcal{H}^{(n_y)}|\Psi_8\rangle$
10. measure final state in computational basis
 $|\Psi_9\rangle \stackrel{?}{=} |0^{(n_x)}\rangle \otimes |0^{(n_y)}\rangle \otimes |1\rangle \otimes |1\rangle$

The algorithm fails when measurement of one of the ancilla qubits yields $|0\rangle$, i. e., if the photon is absorbed or if a projection onto the wrong k -values is performed.

The probability of obtaining $|1\rangle$ as the result of the last measurement corresponds to the probability of template matching, i. e., given a template such as the letter **A** and an initial state such as the (noise-perturbed) state $|B\rangle$, the quantum algorithm decides whether the template is

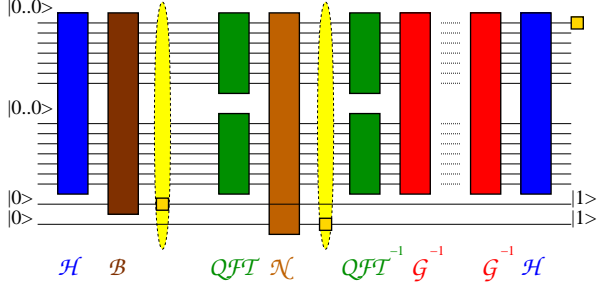


FIG. 2: [Color Online] Quantum circuit of the template matching algorithm for 14 control qubits (7 for x and y respectively) plus 2 ancilla qubits (ancilla qubit values shown for a successful run).

matched or not. Note that due to the finite accuracy of the (discrete) Grover iterations, the algorithm does not terminate with probability 1 in the state $|0^{(n_x)}\rangle \otimes |0^{(n_y)}\rangle$ – even for perfect image-template matches. This state is only be approximated, see also figure 3. Note however, that there exist modifications of Grover’s algorithm that allow for a perfect rotation (compare e. g., [16]). Interestingly, the accuracy of the discretization approximation is the better, the smaller and thinner the letter is, i. e., the smaller M_{tp} . In reality however, this feature would probably be destroyed by imperfections due to the increased required number of Grover iterations.

VI. ALGORITHMIC PERFORMANCE

Starting from a possibly perturbed initial state as prepared by step 3 of the quantum algorithm, we have numerically simulated the action of the corresponding unitary matrices and measurements. As the number of allowed states increases exponentially with the number of simulated n qubits, the numerical simulations would involve $2^n \times 2^n$ matrices which do not fit into the main memory. Fortunately, the involved unitary operations can be expanded into combinations of one or two qubit operations [8], which can be calculated. Thus, the whole algorithm for pattern recognition for 18 qubits runs in a time of few seconds. As a noisefilter function a sharp cutoff was used, i. e.,

$$\vartheta(k_x, k_y) = \begin{cases} 0 & : 0 < \sqrt{k_x^2 + k_y^2} < k_{\max} \\ \pi/2 & : \text{otherwise} \end{cases}, \quad (8)$$

which leads to a simple projection on the allowed k -values. In addition to the high-frequency ($k \geq k_{\max}$) components, it can be advantageous to remove the $k_x = k_y = 0$ component as well, especially if the noise significantly changes the total number of points in the image.

The computational complexity of the algorithm depends on the total number of pixels and on the number of points in the template. The Hadamard gates and the quantum controlled refractors require $\mathcal{O}\{n_x + n_y\}$

operations and the quantum Fourier transforms involve $\mathcal{O}\{n_x^2 + n_y^2\}$ gates. The necessary number of Grover iterations depends on the size of the template $R = \mathcal{O}\{\sqrt{N_x N_y / M_{tp}}\}$, and the number of involved gates per Grover iteration depends on the physical realization of the oracle function $f(x, y)$. Many template points (e. g., bold and large letters) lower the number of required Grover iterations.

Similarly, one has to estimate the failure probability, i. e., how often one of the ancilla bits yields zero. The probability for the photons to be reflected (first ancilla) is given by the ratio of the image size (number of points) over the total area of the array (number of pixels), i. e., many image points are favorable (similar to the above point). For the second ancilla the failure probability depends on the amplitudes of the removed k -values and thus roughly on the amount of noise and the number of fine details in the image.

For specific templates we have made our algorithm explicit: With a given template **A** or **B** (cf. figure 3 top panels), we numerically calculated the recognition probability for all the possible combinations (image **A** and template **B** etc.) for various noise levels (cf. figure 3 lower panels).

We define the recognition ability as the capability of the algorithm to recognize a template state as the corresponding template, whereas the discrimination ability denotes the capability of the quantum algorithm to distinguish between the alternatives in the given alphabet **A**, **B**, see figure 4. A rough measure for the discrimination ability is given by the difference between the acceptance probability when the input state corresponds to the template (circle symbols) and the acceptance probability when the input state does not match the template (square symbols). Trivially, the matching capability deteriorates with increased distortion. For this example, the apparent asymmetry in matching **A** and **B** results from the different numbers of image points occupied by the two templates, as has been checked by applying the algorithm to a different (more symmetric) font. Usually, a performed Fourier cutoff should slightly deteriorate acceptance probability of perfect matches between template and the initial state. However, in figure 4 one can see that this is not the case for the **B-B** configuration (compare large and small circle symbols). This is due to the comparably large number of image points for the chosen font template **B**, which in turn leads to a poor accuracy of the two required Grover iterations. Most important, one can see that even for distorted images (compare with figure 3), the discrimination capability is kept at large values if a Fourier noisefilter is applied. In contrast, if no noisefiltering is used, the discrimination ability decreases rapidly with noise present.

Note that the algorithm is vulnerable to translation, i. e., it does not recognize an image that has been translated in position space compared to the template. To cope with translations, it is necessary to use more than one reflected photon and to analyze the two-photon cor-

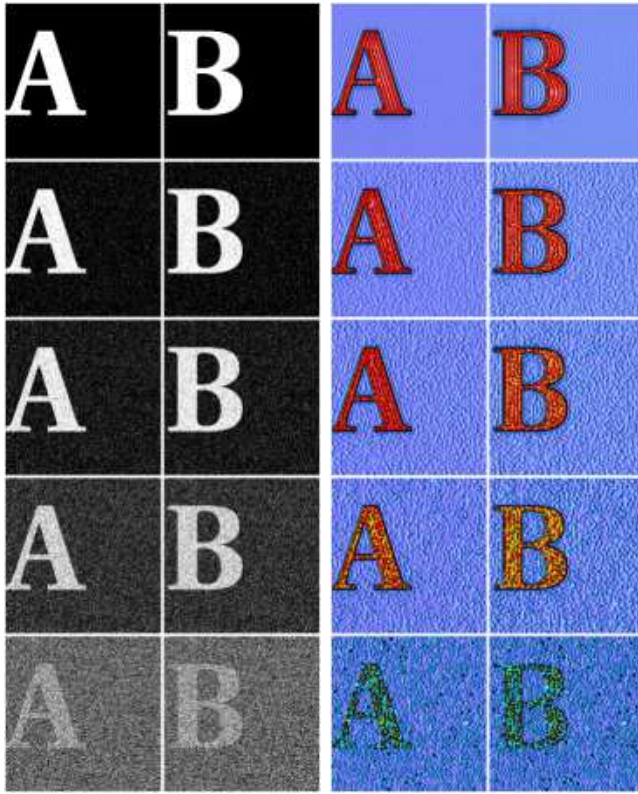


FIG. 3: [Color Online] **Left:** Images of the input states (512×512) with various noise levels. From top to bottom the image pixels of the initial state have been inverted with a probability of 0%, 5%, 10%, 20%, and 40%, respectively. **Right:** Panels show the distribution of the squared amplitude of the inverse of the Fourier-smoothed images (i. e., after step 6 of the quantum algorithm). Only k -values with $0 < k < 40$ have been kept. All amplitudes larger than half the maximum amplitude in every image are shown in red, whereas the thin black isoline encodes the quarter of the maximum amplitude.

relations. After determining the center of mass of the image, for example, one could perform the same algorithm with a template that has been shifted accordingly.

Since the objective is to shine as few photons as possible onto the image, one should try to extract as much information as possible from single measurements. Unfortunately, after a complete measurement of all the qubits separately, the full quantum state has been projected onto the outcome and no information is left. However, in order to accept or reject the hypothesis of a given template, we do not need to measure all the qubits. It is completely sufficient to ask the questions “Are *all* the (non-ancilla) qubits in the state $|0\rangle$ or not?” (Are the non-ancilla qubits in the state $|0\rangle$ of the computational basis?) Alternatively, one could also construct a unitary operator (as with the noisefilter operator \mathcal{N}) that uses an ancilla qubit to answer this question. If the answer by measurement is “yes”, we have accepted the hypothesis (probabilistically) and the full quantum state has been projected onto the state $|0\rangle \otimes |11\rangle$. However, if the an-

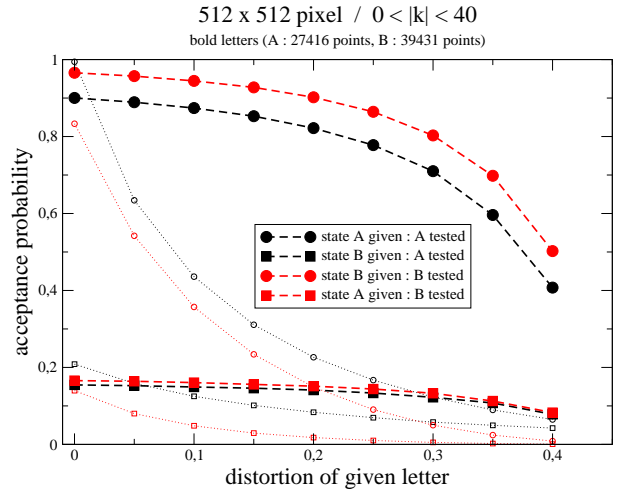


FIG. 4: [Color Online] Probability to recognize the initial state as the template versus noise level. Small hollow symbols represent results without noisefilter applied.

swer is “no” and we have rejected the hypothesis (again probabilistically), the quantum state has only partially been projected onto the high-dimensional sub-space orthogonal to $|0^{(n_x)}\rangle \otimes |0^{(n_y)}\rangle$ and still contains a significant amount of information.

For example, let us assume that we performed the algorithm with the template **A** and that this hypothesis has been rejected, i. e., not all of the qubits were in the state $|0\rangle$. One possibility for this rejection would be that the input state was $|B\rangle$ (rejection correct) or that an input state $|A\rangle$ was falsely rejected (either due to strong perturbations or just due to the inherent probabilistic nature, see figure 4). In this case, we can partially undo the operations specific to template **A** by applying a Hadamard gate onto each qubit again and Grover-rotating back with the template **A**. Now we may switch to the template **B** and perform the inverse Grover rotation with the new template **B** plus the Hadamard gates and measure the outcome. In case the overlap between the images **A** and **B** is small enough, the result of this measurement indicates whether the image is probably **B** and the rejection of **A** was correct or whether something else happened (e. g., the rejection was erroneous or the image is neither **A** nor **B**).

Thus, if the first template had $M_{\text{tp}}^{(1)}$ points and the second template had $M_{\text{tp}}^{(2)}$ points, we could continue the quantum algorithm as follows

11. apply Hadamard gates on non-ancilla qubits
 $|\Psi_{11}\rangle = \mathcal{H}^{(n_x)} \otimes \mathcal{H}^{(n_y)} |\Psi_{10}\rangle$
12. perform $R = \left[\frac{\pi}{4} \sqrt{N_x N_y / M_{\text{tp}}^{(1)}} \right]$ Grover iterations with respect to template **A**
 $|\Psi_{12}\rangle = \mathcal{G}_A^R |\Psi_{11}\rangle$

13. switch to the second template **B** and perform

$$R' = \left[\frac{\pi}{4} \sqrt{N_x N_y / M_{\text{tp}}^{(2)}} \right] \text{ inverse Grover iterations}$$

with respect to template **B**

$$|\Psi_{13}\rangle = \mathcal{G}_B^{-R'} |\Psi_{12}\rangle$$

14. apply Hadamard gates on non-ancilla qubits

$$|\Psi_{14}\rangle = \mathcal{H}^{(n_x)} \otimes \mathcal{H}^{(n_y)} |\Psi_{13}\rangle$$

15. measure final state in computational basis

$$|\Psi_{15}\rangle \stackrel{?}{=} |0^{(n_x)}\rangle \otimes |0^{(n_y)}\rangle \otimes |1\rangle \otimes |1\rangle$$

The measurement at step 10 of the quantum algorithm essentially subtracts the template **A** from the state. Consequently, in case of a false rejection, the state amplitudes will concentrate on the perturbations of the image and the interference patterns resulting from the Fourier noisefiltering, see figure 5 left panels. Consequently, the resulting state is then nearly orthogonal to the second hypothesis in general. In case of a correct rejection of the first hypothesis, the state's squared amplitudes will decrease where the state overlaps with the first template, see figure 5 right panels. Note that here also the different magnitudes of the amplitudes due to the different number of points will in most cases prohibit a complete removal of these amplitudes. In this case, the overlap between the state and the second template will be substantial.

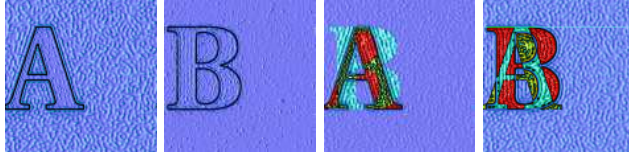


FIG. 5: [Color Online] Color-coded distribution of the squared amplitudes of the state after step 12 of the quantum algorithm (rejection of the first hypothesis). Color-coding has been chosen as in figure 3 and all images have been perturbed by 5% initially. From left to right, the combinations have been chosen as follows: (image **A**, template **A**), (image **B**, template **B**), (image **A**, template **B**), (image **B**, template **A**).

In this second attempt, the recognition probability for a correct hypothesis is naturally smaller as if the second hypothesis had been tested directly, see large versus small symbols in figure 6. However, this procedure has the advantage, that no further interaction with the image is necessary. A further important advantage is that the probability of falsely recognizing a template is extremely low (large circle symbols in figure 6). This is due to the small overlap of the second hypothesis template and the falsely rejected state vector (compare again figure 5 left panels). Consequently, in alphabets containing only few letters, one can identify the letter with a reasonable probability and detect false rejections with high probability – with just a single reflected photon. Note however, that this does not detect falsely accepted hypotheses in the first run.

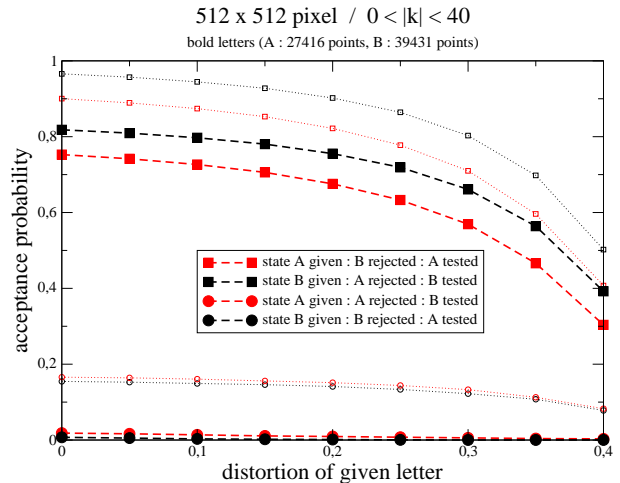


FIG. 6: [Color Online] Probability for acceptance of the second hypothesis after rejection of the first one. For comparison, the small hollow symbols (same data as large symbols in figure 4) – corresponding to the acceptance probability if the second hypothesis had been tested as the first one – have been included.

VII. DISCUSSION AND SUMMARY

We have demonstrated that a quantum computer would be far more effective than a classical computer in template recognition – especially if non-destructive measurements on sensitive systems are to be performed. In the best case, a single photon will suffice to identify a pattern. Even when one takes the finite success probability of the quantum algorithm into account, it still constitutes a major advantage in contrast to classical pattern recognition. Interestingly, the number of qubits required to run the quantum algorithm on an $2^{n_x} \times 2^{n_y}$ image is $n_x + n_y + 2$, e. g., for an 32×32 array only 12 qubits would be required. In case of hypothesis rejection, the algorithm can be used to test a different hypothesis without necessitating a further photon interacting with the quantum array. (Interestingly, the probability of falsely recognizing an input state as the template is much lower in these secondary trials than in the first ones.)

Note that the measurements required during the quantum algorithm can also be performed at the end. In case of a successful run, the photon will not have disturbed the image. In this sense, the quantum algorithm realizes an destruction-free measurement (though probabilistically), which is similar to the Elitzur-Vaidman problem [5].

However, we have only discussed the algorithm from a theoretical point of view, neglecting many imperfections: For example, we did not discuss the experimental difficulties that are to be expected during an experimental implementation of the required quantum circuit. Especially the preparation of the initial state (more specifically, the realization of the quantum-controlled refractors) poses serious problems. In addition, we did not consider the finite accuracy for experimental implemen-

tations of unitary operations on quantum states. Though the implementation of a quantum Fourier transform with optical qubits has been realized, it is very challenging to construct quantum oracles of necessary size.

Despite of these shortcomings, we hope that the presented theoretical discussion of the amazing potential of quantum computers will further contribute to the theoretical as well as experimental developments in this fascinating area.

VIII. ACKNOWLEDGMENTS

This work was supported by the Emmy Noether Programme of the German Research Foundation (DFG) under grant No. SCHU 1557/1-1/2.

[1] P. W. Shor, SIAM J. Comp. **26**, 1484 (1997).
 [2] L. K. Grover, Phys. Rev. Lett. **79**, 325 (1997).
 [3] D. Deutsch Proc. Roy. Soc. Lond. A **400**, 97, (1985).
 [4] D. Deutsch and R. Jozsa, Proc. Roy. Soc. Lond. A **439**, 553, (1992).
 [5] A. C. Elitzur and L. Vaidman, Found. Phys. **23**, 987, (1993).
 [6] D. R. Simon, SIAM J. Comput. **26**, 1474–1483, (1997).
 [7] , E. Bernstein and U. Vazirani, SIAM J. Comput. **26**, 1411–1473, (1997).
 [8] M. A. Nielsen and I. L. Chuang, *Quantum Computation and Quantum Information* (Cambridge University Press, Cambridge, 2000).
 [9] L. M. K. Vandersypen *et al.*, Nature **414**, 883 (2001).
 [10] K. Fukunaga, *Introduction to Statistical Pattern Recognition*, (Academic Press, New York, 1972).
 [11] D. Horn and A. Gottlieb, Phys. Rev. Lett. **88**, 018702, (2002).
 [12] D. Curtis and D. A. Meyer, Proc. SPIE , Quant. Comm. Quant. Imag. **5161**, 134–141, (2004).
 [13] C. A. Trugenberger, Phys. Rev. Lett. **87**, 067901, (2001); Phys. Rev. Lett. **89**, 277903, (2002); [arXiv:quant-ph/0210176], (2002).
 [14] M. Sasaki, A. Carlini, and R. Jozsa, Phys. Rev. A **64**, 022317, (2001); M. Sasaki and A. Carlini, Phys. Rev. A **66**, 022303, (2002).
 [15] R. Schützhold, Phys. Rev. A **67**, 062311 (2003).
 [16] G. L. Long, Phys. Rev. A **64**, 022307, (2001).